



**HAL**  
open science

# Comparative study on different coals from the Lorraine basin (France) by sorption isotherms, thermogravimetric analysis and breakthrough curves for CO<sub>2</sub>-ECBM recovery

Franck Amoïh, Gisèle Finqueneisel, Thierry Zimny, Sandrine Bourrelly, Odile Barres, Dragan Grgic

## ► To cite this version:

Franck Amoïh, Gisèle Finqueneisel, Thierry Zimny, Sandrine Bourrelly, Odile Barres, et al.. Comparative study on different coals from the Lorraine basin (France) by sorption isotherms, thermogravimetric analysis and breakthrough curves for CO<sub>2</sub>-ECBM recovery. *International Journal of Coal Science & Technology*, 2024, 11, pp.46. 10.1007/s40789-024-00696-8 . hal-04611018

HAL Id: hal-04611018

<https://hal.science/hal-04611018v1>

Submitted on 28 Jun 2024

**HAL** is a multi-disciplinary open access archive for the deposit and dissemination of scientific research documents, whether they are published or not. The documents may come from teaching and research institutions in France or abroad, or from public or private research centers.

L'archive ouverte pluridisciplinaire **HAL**, est destinée au dépôt et à la diffusion de documents scientifiques de niveau recherche, publiés ou non, émanant des établissements d'enseignement et de recherche français ou étrangers, des laboratoires publics ou privés.



Distributed under a Creative Commons Attribution 4.0 International License



# Comparative study on different coals from the Lorraine basin (France) by sorption isotherms, thermogravimetric analysis and breakthrough curves for CO<sub>2</sub>-ECBM recovery

Franck Amoih<sup>1</sup> · Gisèle Finqueneisel<sup>2</sup> · Thierry Zimny<sup>2</sup> · Sandrine Bourelly<sup>3</sup> · Odile Barres<sup>1</sup> · Dragan Grgic<sup>1</sup>

Received: 4 June 2023 / Revised: 21 September 2023 / Accepted: 24 April 2024  
© The Author(s) 2024

## Abstract

The enhanced coalbed methane recovery using CO<sub>2</sub> injection (CO<sub>2</sub>-ECBM) is widely proposed as a way of achieving the energy transition and reducing atmospheric CO<sub>2</sub> in areas such as the Lorraine basin in France, where heavy industry is responsible for huge CO<sub>2</sub> emissions and coal mines have been closed for more than a decade. This paper deals with the feasibility of extracting methane from the Lorraine basin using CO<sub>2</sub>-ECBM by comparing data from sorption isotherms, thermogravimetric analyses and breakthrough curves for two coal samples. One is bituminous (Box 18), from Folschviller (France) and is compared with another sub-bituminous (TH01) from La Houve (France), which is used as a reference because it was identified as a good candidate for CO<sub>2</sub>-ECBM in a previous research program. The quantities of adsorbed gases (CO<sub>2</sub>/CH<sub>4</sub>) obtained by sorption isotherms, thermogravimetry and CO<sub>2</sub> breakthrough curves showed that Box 18 adsorbs more CO<sub>2</sub> and CH<sub>4</sub> than TH01 due to its higher porosity and good affinity for gases (CO<sub>2</sub>/CH<sub>4</sub>). Tóth model fits the experimental CH<sub>4</sub> and CO<sub>2</sub> adsorption isotherms better, reflecting the fact that the adsorption surface of the coals studied is heterogeneous. Adsorption enthalpies obtained by calorimetry indicated physisorption for gas-coal interactions, with higher values for CO<sub>2</sub> than for CH<sub>4</sub>. Thermogravimetric analyses and breakthrough curves carried out at up to 50% relative humidity showed that the adsorption capacity of CO<sub>2</sub> decreases with increasing temperature and the presence of water, respectively. The compilation of these experimental data explained the adsorption process of the studied coals and revealed their advantages for CO<sub>2</sub>-ECBM.

## Highlights

- The Folschviller coal from Lorraine basin (France) meets the main criteria to be a good candidate for CO<sub>2</sub>-ECBM due to his porosity network, adsorption capacity and affinity for gases (CO<sub>2</sub>/CH<sub>4</sub>).
- The binding energy between the gas and the coal samples is low corresponding to physical adsorption; however, chemical adsorption of CO<sub>2</sub> was detected by thermogravimetry at atmospheric pressure.
- Calorimetry and sorption isotherms modelling showed that the adsorption surface of coal is heterogeneous with a progressive filling of the high energy sites towards the lower energy sites.

---

✉ Dragan Grgic  
dragan.grgic@univ-lorraine.fr

Franck Amoih  
franck-aristide-k.amoih@univ-lorraine.fr

<sup>1</sup> Laboratoire GeoRessources, CNRS, Université de Lorraine, 54500 Vandoeuvre-lès-Nancy, France

<sup>2</sup> Laboratoire de Chimie et de Physique - Approche Multi-échelles des Milieux Complexes (LCP-A2MC-EA 4632), Université de Lorraine, 57500 Saint-Avold, France

<sup>3</sup> Laboratoire MADIREL, CNRS-UMR7246, Université Aix-Marseille, Centre de St Jérôme, 13397 Marseille Cedex 20, France

- The breakthrough curves and thermogravimetry carried out at atmospheric pressure showed respectively that water and temperature reduce the CO<sub>2</sub> adsorption capacity of coals.

**Keywords** CO<sub>2</sub>-ECBM · Geological storage · Adsorption capacity · Coal

## 1 Introduction

Natural gas from coal formation is emerging as a clean energy solution with increasing production in recent years (Hayes and Roeshot 2014). In addition, underground sequestration of greenhouse gases is emerging as a means to combat global warming (Metz et al. 2005). The challenge to be met today for the preservation of the environment would be to couple both the exploitation of methane and the secure storage of CO<sub>2</sub>. The main candidates for underground CO<sub>2</sub> storage are former hydrocarbon reservoirs (oil or gas), saline aquifers and unmineable, overdeep coal seams. The latter are very interesting for the advantages they offer, e.g., wide geographical distribution, financial benefit of methane recovery and good chemical affinity between CO<sub>2</sub> and coal that guarantees safe storage.

The most studied coal seams for CH<sub>4</sub> recovery by CO<sub>2</sub> injection are located in Australia, China, India, Russia and the USA, representing more than 70% of the world's coal reserves (Li and Fang 2014; Pashin et al. 2001; White et al. 2005). Furthermore, CO<sub>2</sub> storage in coal seams is viable over long geological time periods (White 2003). This is because coal adsorbs CO<sub>2</sub> molecules to its surface in a stable manner and the high affinity of coal for CO<sub>2</sub> ensures the stability of the coal–CO<sub>2</sub> bond, thus limiting the risk of leakage very considerably (Clarkson and Bustin 1999). As a result, this type of CH<sub>4</sub> exploitation has the potential to become a profitable business model, including feasibility, reduced CO<sub>2</sub> storage costs through CH<sub>4</sub> recovery and societal acceptance due to limited risks. Regarding its storage potential, coal can, due to its high affinity for CO<sub>2</sub> and its specific surface area (20 to more than 300 m<sup>2</sup>/g), store between 40 and 60 m<sup>3</sup> of CO<sub>2</sub> per ton of coal, at gas pressures of 5–6 MPa (Mahajan 1991; Marsh 1987). A global survey of several previous works and ECBM pilot sites indicate that it is possible to store up to 200 Gt of CO<sub>2</sub> in coal for a volume of 50 trillion m<sup>3</sup> of CH<sub>4</sub> recovered (Godec et al. 2013; Metz et al. 2005; Ottiger et al. 2006).

The exploitation of natural gas in coal is carried out either conventionally or artificially. In the first case, the gas rises naturally to the surface with the pressure gradient between the coal in the sub and the atmospheric pressure. This technique allows 20%–60% of the methane to be recovered. The unconventional method, known as ECBM, involves creating a pressure gradient through dewatering, hydraulic fracturing or fluid injection. The methane rises to the surface as a result of a drop in its partial pressure in the underground coal.

Dewatering and fluid injections are much more widely used by industry because they are more societally acceptable. The gases used in fluid injection to recover methane are N<sub>2</sub>, CO<sub>2</sub> or a mixture of both. In the case of CO<sub>2</sub>, this exploitation technique is known as CO<sub>2</sub>-ECBM. Injecting CO<sub>2</sub> into the coal generates and maintains a pressure gradient. On the other hand, it reduces the partial pressure of the methane, which desorbs from the coal matrix and flows through the fractures to the extraction well. The CO<sub>2</sub> injected into the coal is then adsorbed, thus reducing its presence in the atmosphere and the risk of global warming, while the methane extracted from the coal will be used as an energy source. Although it has been estimated that burning one ton of CH<sub>4</sub> can produce 2.27 tons of CO<sub>2</sub>, there would be a net storage of CO<sub>2</sub> from a carbon balance in a CO<sub>2</sub>-ECBM operation even if all the CH<sub>4</sub> recovered is burnt (Ottiger et al. 2006).

CO<sub>2</sub> storage associated with CH<sub>4</sub> recovery (CO<sub>2</sub>-ECBM) has been studied through the many pilot sites around the world (San Juan basin in USA, Ishikari coal basin in Japan, Silesian coal basin in Poland, Bowen basin in Australia, Qinshui basin in China, etc.) (Li and Fang 2014). This led to the acquisition of information on the physico-chemical processes that could occur during CO<sub>2</sub>-ECBM operation. These processes are Darcean gas flow in the fractures, diffusion (Fick's law) of the gas in the coal matrix, adsorption/desorption, dissolution of CO<sub>2</sub> in the coal water, compression of the coal matrix and skeleton, and swelling/shrinking of the coal which will alter the permeability in the reservoir and induce changes in injection pressures. All these processes are influenced by temperature, CO<sub>2</sub> injection pressure, in situ stresses, rank and coal moisture (Mukherjee and Misra 2018; Shi and Durucan 2005). The matrix of coals has a network of pores of different diameters that facilitates the circulation of CO<sub>2</sub> through the coal matrix. The porous network of coals include micropores (0.0008–0.0020 μm) next to which there are macropores (> 0.05 μm) and mesopores (0.002–0.050 μm) (Gan et al. 1972; IUPAC 1972; Parkash and Chakrabarty 1986; Sing 1995). It is therefore important to evaluate the following parameters in order to carry out a CO<sub>2</sub>-ECBM operation successfully: gas adsorption capacity limit (CO<sub>2</sub>/CH<sub>4</sub>), CH<sub>4</sub> recovery rate, matrix volumetric deformation, state of fracturing, pore distribution, matrix compressibility, porosity and permeability of the coal seam. The assessment of the storage potential of the coal seam is based on the study of these physicochemical parameters and its geological characteristics. It should be noted that the selection of one or more coal seams for CO<sub>2</sub>-ECBM mining

is the starting point and the key to the success of the project. Therefore, this selection requires further knowledge of the adsorption/desorption processes and their interactions with other physico-chemical processes likely to occur during a CO<sub>2</sub>-ECBM operation because coals have different internal structures (fracturing, macerals, and specific surface area due to the difference in maturity and geological conditions of the seam in situ depth, temperature and pressure) (Liu et al. 2018; Okolo et al. 2015). This selection should be carried out using all available techniques and tools. Each of them has its advantages and limitations. Nevertheless, the combination of these techniques would provide a maximum of information.

The present study is part of the REGALOR (Gas Resources of Lorraine) project and deals with the selection of a coal suitable for CO<sub>2</sub>-ECBM exploitation based on data obtained by different techniques and analysis tools. This is a research and development project which aims to evaluate the gas reserves of the Lorraine region (France) subsoil and to optimize their recovery while controlling and minimizing the environmental impact. The samples studied come therefore from the Lorraine coal basin (France). The Lorraine coal deposits contain an unconventional gas resource (mainly CH<sub>4</sub>) estimated at 370 billion m<sup>3</sup> (Gunzburger 2016). Therefore, they constitute an important asset in the energy independence policy of France and Europe for the next decade. Although the CH<sub>4</sub> resource in the Lorraine basin is available, it is also important to investigate its suitability for underground CO<sub>2</sub> storage. The complex and heterogeneous nature of coal means that the gas-coal interaction mechanism and the gas adsorption process (CO<sub>2</sub>/CH<sub>4</sub>) on a given type of coal during CO<sub>2</sub>-ECBM operations need to be investigated specifically. This study therefore focuses on assessing the suitability of coals from Lorraine for CO<sub>2</sub>-ECBM operations. It deals with the adsorption process of Lorraine coal and the influence of factors such as temperature and humidity. In this paper, two coal samples are compared. The first one (from La Houve) has already been identified by Defosse (2011) as suitable for CO<sub>2</sub>-ECBM. The second one (from Folschviller) will be analyzed to determine whether or not it is also qualified. After a comparison of samples from Europe (France, Spain, Poland, Sardinia), South America (Colombia) and Africa (Morocco), Defosse (2011) also defined criteria that a coal must have to be a good candidate for the CO<sub>2</sub>-ECBM, namely the ash content, the adsorption capacity and the affinities of the gases (CO<sub>2</sub>/CH<sub>4</sub>) with the coal.

For this purpose, conventional characterization techniques such as rock-*eval* pyrolysis, petrographic analysis and mercury porosimetry were used to assess the rank, maceral composition and distribution of pores in the samples, with a view to comparing their overall physico-chemical properties

with gas adsorption data (CO<sub>2</sub>/CH<sub>4</sub>). Several techniques for analyzing gas adsorption on coals were used in this research work, each with a well-defined field of study. These are sorption isotherms, break-up curves and thermogravimetric analysis. Sorption isotherms coupled with calorimetry were used to assess the quantities of CO<sub>2</sub> and CH<sub>4</sub> adsorbed and the gas-coal binding of coal samples. Breakthrough curves were used to study the influence of water on adsorbed CO<sub>2</sub> quantities. Thermogravimetric analyses were used to study the influence of temperature on CO<sub>2</sub> adsorption of the samples studied (adsorption capacities and kinetics). Fourier transform infrared reflectance spectroscopy (DRIFT) was used to study the distribution of oxygen-containing functional groups, aromatic hydrocarbons and aliphatic groups in the selected coal samples. A qualitative analysis of the functional groups during CO<sub>2</sub> adsorption and also in the presence of moisture was carried out to study their behavior in the presence of CO<sub>2</sub> and H<sub>2</sub>O molecules.

## 2 Materials and methods

### 2.1 Coal samples

The coal samples studied belong to the Lorraine basin (Fig. 1). The first one comes from the Folschviller borehole (REGALOR pilot site, Grand Est, France) while the second one is from the La Houve mine (Grand Est, France). The Folschviller borehole intersects 10 coal seams with a thickness of between 4 and 16 m. For this study, the thickest seam was chosen because it is likely to store the most CO<sub>2</sub>. It corresponds to the sample named Box 18 extracted from a borehole at 817 m. The La Houve coal sample named TH01 is from the Albert vein located at a depth of approximately 900 m.

### 2.2 Coal characterization methods

#### 2.2.1 Proximate, ultimate and petrographic analyses

The elemental composition (carbon, hydrogen, oxygen and sulfur) in coal was determined by analyser (Elementar Vario Micro Cube). This organic elemental analyser is based on the principle of safe, simple and environmentally friendly high-temperature combustion with furnace temperatures well above 1000 °C; guaranteeing a complete quantitative conversion of the sample into the measurement gas for highly accurate elemental analysis. It contains chromatographic gas separation columns and detectors. These include a thermal conductivity detector (TCD), an infrared detector for sulphur and oxygen and an electrochemical detector for chlorine.



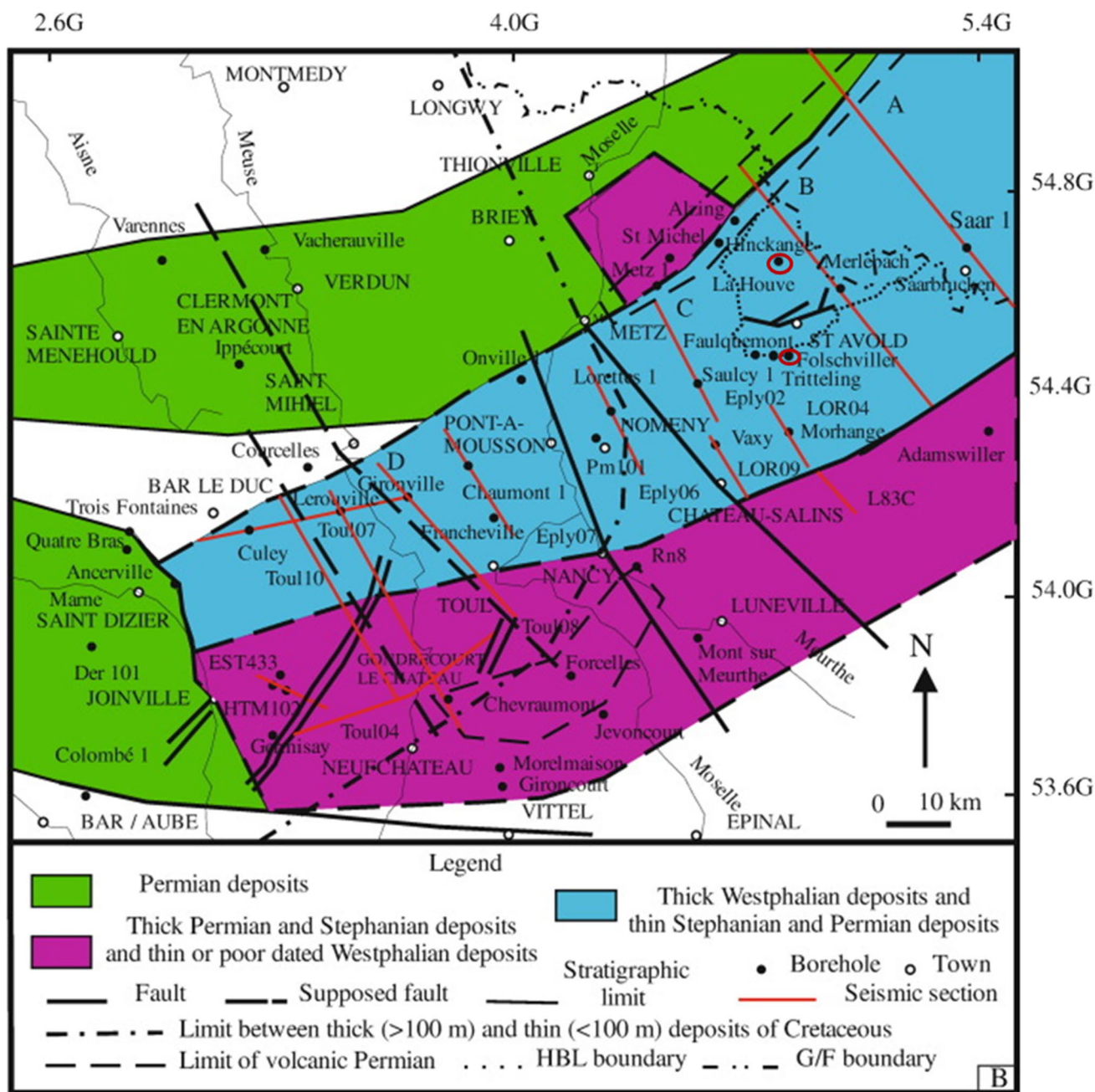


**Fig. 1** Geological map of the Carboniferous and Permian basins with the location of the coal samples studied (borehole circled in red) modified from (Izart et al. 2016). A Armorican zone, G/F Germany/France, HBL Lorraine Coal Basin concession, L Lorraine Coal Basin,

LA Liguro-Arverne zone, M Moldanubian zone, MGH Mid-German High, RH Rheno-Hercynian zone, S Saar coal Basin, ST Saxo-Thuringian zone, V Vosges, VF Hercynian foredeep

The ash content of the samples studied was obtained by following the French standard NF M 03-003. The volatile matter index is obtained according to the AFNOR MO3-004 standard. Total organic carbon (TOC) and  $T_{max}$  were carried out with 20–30 mg of coal powder (particle size < 200 μm), with a Rock-Eval® 6 from Vinci Technologies, under standard conditions (Lafargue et al. 1998). The petrographic composition, mineral matter content and vitrinite reflectance of

coals were estimated following standard procedures as well as ICCP recommendations.

### 2.2.2 Determination of pore volume

Mercury porosimetry analyses were carried out on a coal cubic block of about 1 cm<sup>3</sup> to determine the Hg connected (total), free and trapped porosity, the pores size distribution

and the coal density. The total porosity ( $n_t$ ) is calculated from the volumetric mass densities as follows:

$$n_t = \left( 1 - \left( \frac{\rho_d}{\rho_s} \right) \right) \times 100 \quad (1)$$

where  $\rho_d$  is the bulk dry density of obtained on a cylindrical core sample of coal of about 80 cm<sup>3</sup> and  $\rho_s$  is the density of the solid matrix of coal powder (particle size < 80 μm) obtained with the Helium pycnometer. Note that the densities were obtained on oven-dried coal samples at 60 °C. The AccuPyc II 1340 (Micromeritics, Inc.) was used to estimate the solid matrix density with Helium by measuring the change of pressure in a calibrated volume. Helium adsorption on coals was assumed to be non-existent or negligible.

## 2.3 Infrared spectroscopy

### 2.3.1 Diffuse reflectance infrared spectroscopy

Infrared spectra were carried out using a BRUKER IFS 55 Fourier transform infrared spectrometer equipped with a liquid nitrogen cooled MCT (mercury-cadmium-telluride) detector. The diffuse reflectance (DRIFT) spectra were collected with a diffuse reflectance attachment (Praying Mantis™, Harrick) equipped with an environmental reaction chamber (HVC) with a dome with two ZnSe (zinc selenide) windows and one glass observation window. The reaction chamber is connected to a standard vacuum line and can be operated under pressure from  $5 \times 10^{-7}$  MPa mbar to 0.1 MPa. The spectra were recorded in the mid-infrared range from 5000 to 500 cm<sup>-1</sup> by accumulation of 200 scans at a resolution of 2 cm<sup>-1</sup>. The powdered coal samples (< 80 μm) were analysed with a 15% by weight dilution in KBr (potassium bromide) used as a reference. The particle is inferior to 80 μm to comply with the tool's use and calibration standards. All the coal samples were dried at 60 °C in an oven before the measurements.

### 2.3.2 CO<sub>2</sub> and CH<sub>4</sub> adsorption measurements

The coupling of infrared spectra to CO<sub>2</sub> or CH<sub>4</sub> injections at low pressure and room temperature were carried out to study gas–coal bonding through the chemical functional groups of coal. Standard vacuum line techniques were used to deliver through a stainless steel pipeline the pure CO<sub>2</sub> or CH<sub>4</sub> gas to the powdered coal contained in the reaction chamber described above. The gases were injected at a pressure of 0.17 MPa to saturate the coal sample and the CO<sub>2</sub> or CH<sub>4</sub> remained in contact with the sample for 60 h. Then the sample was released to the atmosphere. Some experiments

have also been performed by introducing water vapor before adsorption of the gases or simultaneously.

## 2.4 Sorption isotherms and gas–coal bonds

The sorption isotherms were used to evaluate the adsorbed quantities of CO<sub>2</sub> and CH<sub>4</sub> on the coal samples. CO<sub>2</sub> and CH<sub>4</sub> sorption isotherms were carried out on a dried coal powder of approximately 1 g with a particle size between 40 and 200 μm by manometric method. The choice of this particle size is based on a study by Charrière (2009), who showed that the larger the grain size, the greater the sorption equilibrium time. In his work, the grain size between 40 and 200 μm had the lowest sorption equilibrium time. Powdered coal samples were dried at 60 °C in an oven before the measurements. These adsorption isotherms were measured at a constant temperature of 30 °C and up to 50 bars. The obtained data were then processed with the Langmuir and Tóth models (Langmuir 1918; Tóth 1962). The gas–coal interactions study consisted in the determination by microcalorimetry of the adsorption enthalpies of CO<sub>2</sub> and CH<sub>4</sub> for the samples Box 18 and TH01. Adsorption microcalorimetry experiments were performed using an in-house built setup that combines manometric dosing system with a high sensitivity Tian–Calvet isothermal type microcalorimeter (Poyet 2002). This apparatus can be thermoregulated at 30 °C and allows both the isotherms and the pseudo differential enthalpies of adsorption as a function of the coverage to be measured simultaneously up to 50 bars. The errors in the isotherms can be considered as better than 5% and errors in the enthalpies are of  $\pm 1$  kJ/mol. The introduction of gas by doses is more adapted to this system (to be able to reach relatively high pressures). The Tian–Calvet type microcalorimeter consists of two thermopiles, each comprising about 500 chromel–alumel thermocouples, mounted in electrical opposition (Calvet and Prat 1958; Rouquerol et al. 1977). All the details of this device and its operation are developed by Llewellyn and Maurin (2005).

## 2.5 Thermogravimetric analyses

Thermogravimetric analyses were used to study the influence of temperature on the adsorption of CO<sub>2</sub> from these samples (adsorption capacities and kinetics). The mass variations of coal subjected to CO<sub>2</sub> and helium flows at constant temperature were followed by TGA apparatus. The measurements were carried out on a mass of about 250 mg of powdered coal (particle size between 40 and

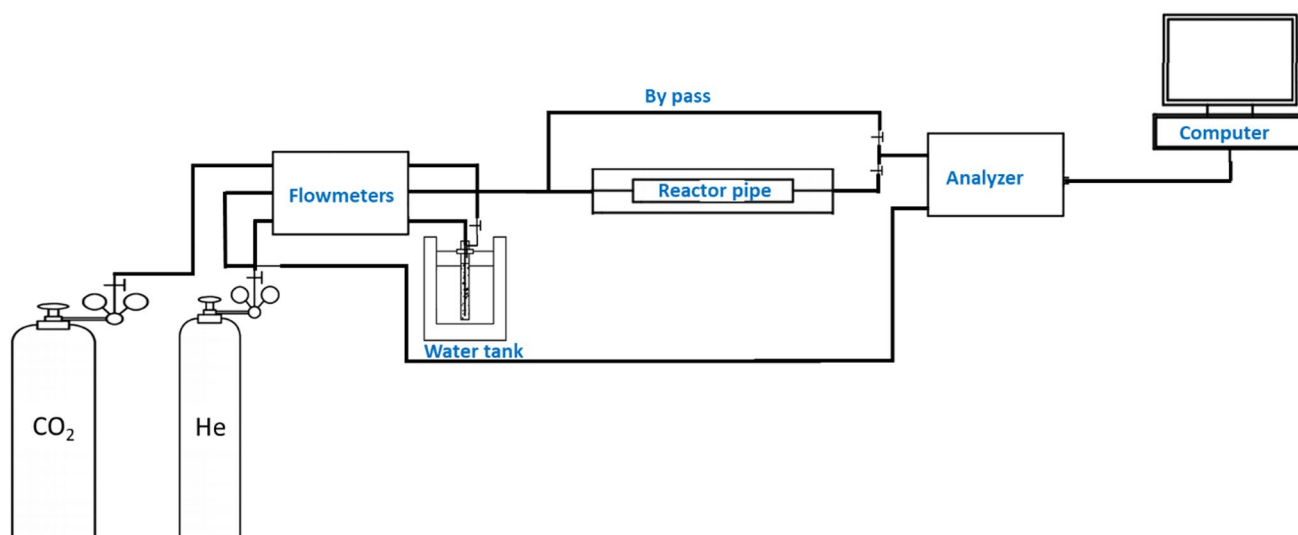


**Fig. 2** Experimental device for the acquisition of breakthrough curves

200  $\mu\text{m}$ ) and at different temperatures between 25 and 85  $^{\circ}\text{C}$ . The granulometry of the coal powder is kept here to be consistent with the sorption isotherms. The measurement cycle includes a first phase where the coal is subjected to a  $\text{CO}_2$  flow followed by a phase where it is subjected to helium. The gas flow rate was set at 50 mL/min. The duration of exposure of the coal to the gas flow during each phase is 30 min. This measurement cycle is repeated twice to assess the reproducibility of the analysis. Before each measurement cycle, the coal is subjected to a helium flow and is heated to 200  $^{\circ}\text{C}$  for 2 h to degas it. The rate of temperature is 10  $^{\circ}\text{C}/\text{min}$ .

## 2.6 Breakthrough curves

The breakthrough curves were used to study the influence of water on the quantities of  $\text{CO}_2$  adsorbed. The analyses were carried out at room temperature under a constant gas flow (25 mL/min) and at different humidity percentages (0%, 10% and 50%).

The principle of the breakthrough curve is based on sending a constant gas flow to a reactor pipe (glass tube containing powdered coal) and monitoring the gas concentrations at the reactor outlet over time. The adsorption reactor consisted of a pipe 50 cm long and 1 cm diameter and two screwed pieces in the extremes. Glass wool confined the fixed bed resulting in a bed height of 30 cm. The particle size of the coal was between 40 and 200  $\mu\text{m}$ . The granulometry of the coal powder is kept here to be consistent as possible with the sorption isotherms. To control the composition of the gas mixture, separate flow controllers are used to adjust the flow rate of different component. A micro gas chromatography

analyzer was used to measure the effluent concentration at the exit of the system (Fig. 2).

Breakthrough curves were performed twice for each sample on approximately 8.5 g of coal. The  $\text{CO}_2$  concentration (purity: 99.99%) was set at 0.4%. The carrier gas used was helium. Before each experiment, the coal was heated to 200  $^{\circ}\text{C}$  for 3 h under a helium flow at a gradient of 10  $^{\circ}\text{C}/\text{min}$  to degas it. After degassing and at room temperature, the coal was pre-humidified for 1 h with a helium flow loaded with  $\text{H}_2\text{O}$ . This humidity was maintained during the experiment by sending the same flow (percentage  $\text{H}_2\text{O}$ ) of water-laden helium onto the coal.

## 3 Results

### 3.1 Coal samples characterization

#### 3.1.1 Physical and chemical properties of coal samples

The coal samples characteristics are listed in Table 1. The parameters most used to determine the rank of a coal are the temperature ( $T_{\text{max}}$ ), the volatile matter (MV), the organic carbon (TOC) and the reflectivity of the vitrinite ( $R_o$ ). According to the classification of Copard (2002), Box 18 (Folschviller) is classified as High Volatile Bituminous coal while TH01 (La Houve) is classified as Sub-bituminous coal. These coals samples were formed during the catagenesis (maturation stage) of the organic matter corresponding to the oil window or the production of liquid hydrocarbons. They are not very mature and rich in volatile matter as evidenced by the  $T_{\text{max}}$  data which are

**Table 1** Characteristics of the coal samples

Parameter	Box 18	TH01
Ultimate analysis		
Carbon (wt% <sub>db</sub> )	44.87	73.68
Hydrogen (wt% <sub>db</sub> )	3.17	6.73
Oxygen (wt% <sub>db</sub> )	10.47	12.24
Nitrogen (wt% <sub>db</sub> )	0.76	1.70
Sulfur (wt% <sub>db</sub> )	0.40	0.33
Proximate analysis		
Ash (wt% <sub>db</sub> )	0.67	4.08
Volatile matter (wt% <sub>db</sub> )	37.00	34.90
TOC (wt% <sub>db</sub> )	45.21	69.69
$T_{\max}$ (°C)	427.00	441.00
Petrographic analysis		
Vitrinite (vol% <sub>mmf</sub> )	57.67	47.48
Liptinite (vol% <sub>mmf</sub> )	14.25	23.52
Inertinite (vol% <sub>mmf</sub> )	26.51	26.98
Mineral matter (vol%)	1.57	2.02
$R_o$	0.78	0.50

TOC: total organic carbon,  $T_{\max}$ : rock eval temperature,  $R_o$ : mean random vitrinite reflectance, (mmf: mineral matter free basis; db: dry basis, wt: weight)

**Table 2** Densities and pore volume of the coal samples

Parameter	Box 18	TH01
Cylindrical specimen		
Masse (g)	103.26	105.05
Volume (cm <sup>3</sup> )	83.50	87.54
$\rho_d$ (g/cm <sup>3</sup> )	1.24	1.20
Powdered sample		
Masse (g)	4.43	4.16
Volume (cm <sup>3</sup> )	2.57	3.33
$\rho_s$ (g/cm <sup>3</sup> )	1.72	1.25
$n_t$ (%)	27.90	4.00

$\rho_d$ : bulk dry density of cylindrical specimen;  $\rho_s$ : density of solid matrix;  $n_t$ : total porosity (coal rock)

around 430 °C and the volatile matter data around 35 wt%. Table 1 shows that the sample with the highest vitrinite (vol%) has the highest amount of volatile matter, which is in good agreement with those of Moroeng et al. (2019). From a maceral point of view, both samples are dominated by vitrinite (> 45 vol%) and inertinite (> 26 vol%). But, Box 18 sample contains the most vitrinite and could therefore be considered as the one with the most micropores and therefore likely to absorb the most CO<sub>2</sub> (Premalal et al. 2014; Zhang and Yang 1999). Ash and sulfur percentages of the two samples are very low (< 5.0%) and (< 0.4%)

**Table 3** Mercury porosities, pore volumes and surface area of samples Box 18 and TH01

Parameter	Box 18	TH01
Hg porosimetry		
Total porosity (%)	8.000	5.600
Free porosity (%)	6.900	5.500
Trapped porosity (%)	1.100	0.100
$V_p$ (cm <sup>3</sup> /g)	0.220	0.020
$\epsilon$ (%)	27.900	2.500
$V_M$ (cm <sup>3</sup> /g)	0.014	0.007
$V_m + V_\mu$ (cm <sup>3</sup> /g)	0.206	0.013
$\rho_{He}$ (dmmf)	1.720	1.220
$\rho_{Hg}$ (dmmf)	1.240	1.190

$V_p$ : pore volume;  $\epsilon$ : helium accessible porosity;  $V_M$ : macropore volume;  $V_m$ : mesopore volume;  $V_\mu$ : micropore volume;  $\rho_{He}$ : density of coal in helium;  $\rho_{Hg}$ : density of coal in mercury, dmmf– dry mineral matter free

respectively and results show no clear correlation between these and the maturity of coal.

### 3.1.2 Characterization of pore structure

Table 2 shows differences in the proportion of porosity in samples Box18 and TH01. The Box18 sample has the highest total porosity (27.9%). A high total porosity ( $n_t$ ) value is a promising asset for a possible CO<sub>2</sub> storage due to the presence of available voids (mainly cracks). It is interesting to note that Folschviller sample has particularly high values compared to the La Houve sample due to the presence of many cracks. It should be noted that several measurements confirm these total porosity data.

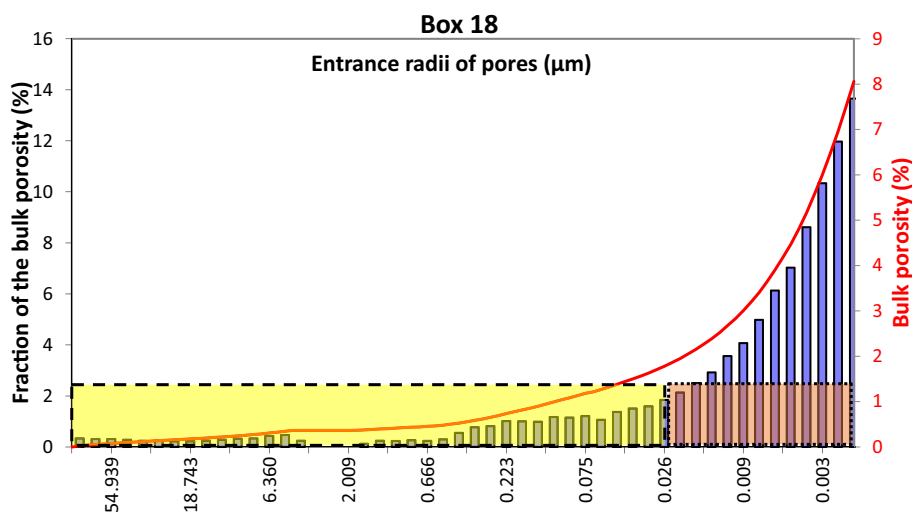
Mercury porosimetry allowed the determination of porosities (total, free, and trapped) and pores size distribution (macropores, mesopores and micropores) and coal density. The mercury total porosity is obtained from the total volume of mercury that penetrates the sample during the first injection. The volume of mercury that penetrate during the second injection is used to determine the free porosity. The difference of these mercury volumes allows calculating the trapped porosity. Indeed, the shape and the network of the material pores do not permit a total recovery of the mercury injected during the first injection. The total volume of open pores is calculated from the Eq. (2).

$$V_p = 1/\rho_{Hg} - 1/\rho_{He} \quad (2)$$

where  $\rho_{Hg}$  and  $\rho_{He}$  are respectively the mercury and helium densities (dmmf for dry mineral matter free). These densities are recalculated by subtracting the ash rate. These densities also allow to calculate the porosity accessible to helium noted  $\epsilon$  via the Eq. (3).



**Fig. 3** Histograms of pore distribution and total porosity of Box 18. Macropores domain is delimited by dashes and mesopores domain is delimited by points



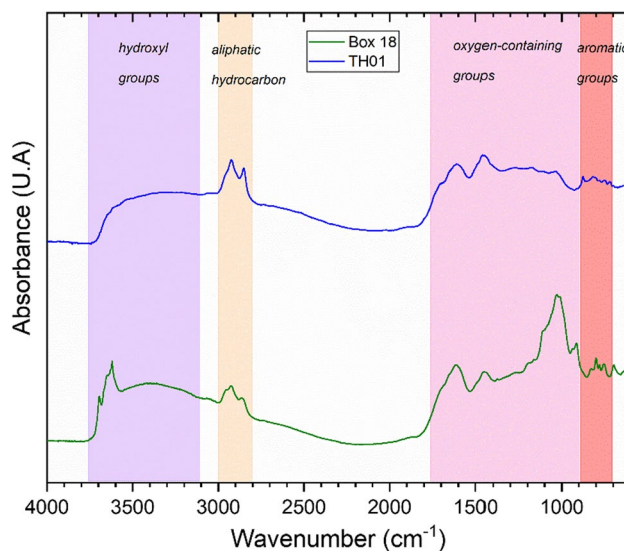
$$\epsilon = 100 * \rho_{Hg} * (1/\rho_{Hg} - 1/\rho_{He}) \tag{3}$$

All the porosity parameters are recorded in Table 3. In this table, the volume of macropores ( $V_M$ ) defines the pores volume with a diameter greater than 0.05  $\mu\text{m}$  saturated with mercury. The sum of the mesopore ( $V_m$ ) and micropore ( $V_\mu$ ) volumes is obtained by the difference between  $V_p$  and  $V_M$ . This sum is derived from the pore classification of (Gan et al. 1972) and the Eq. (4).

$$V_p = V_M + V_m + V_\mu \tag{4}$$

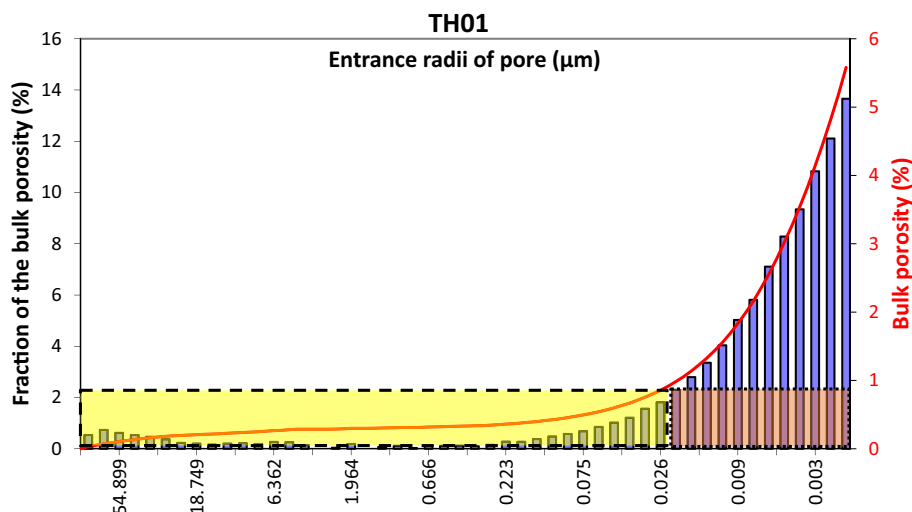
where  $V_M$  is the volume of macropores,  $V_m$  is the volume of mesopores and  $V_\mu$  is the volume of micropores.

Table 3 shows that the mercury and helium accessible porosities of the Folschviller samples are higher than that of the La Houve with the following ranking Box 18 > TH01. The helium accessible porosities of the studied samples are between 2% and 28% and are close to the values obtained by Parkash and Chakraborty (1986) which conclude that



**Fig. 5** IR spectra and functional groups of the studied samples

**Fig. 4** Histograms of pore distribution and total porosity of TH01. Macropores domain is delimited by dashes and mesopores domain is delimited by points



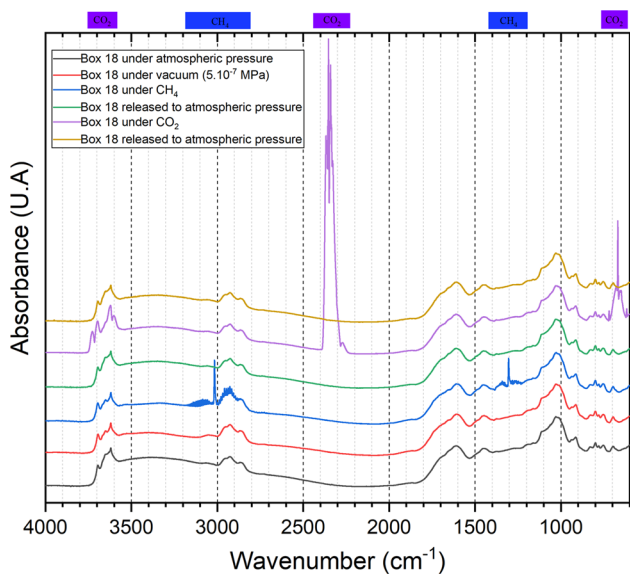


Fig. 6 IR spectra of sample Box 18 under different gas flows (CO<sub>2</sub>, CH<sub>4</sub>) and at atmospheric pressure

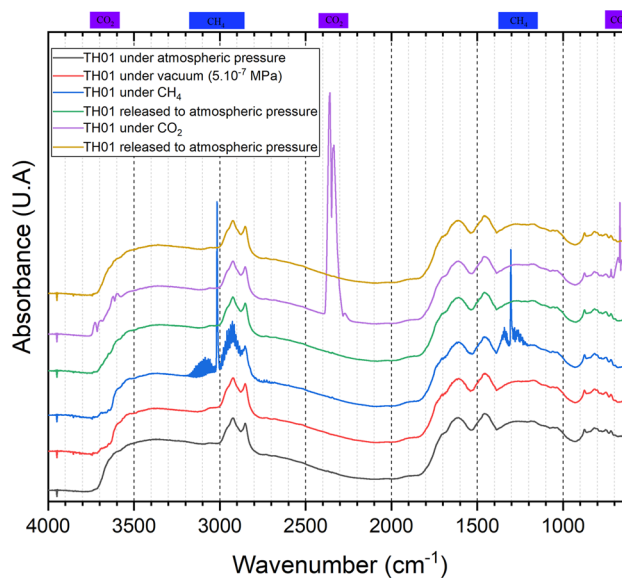
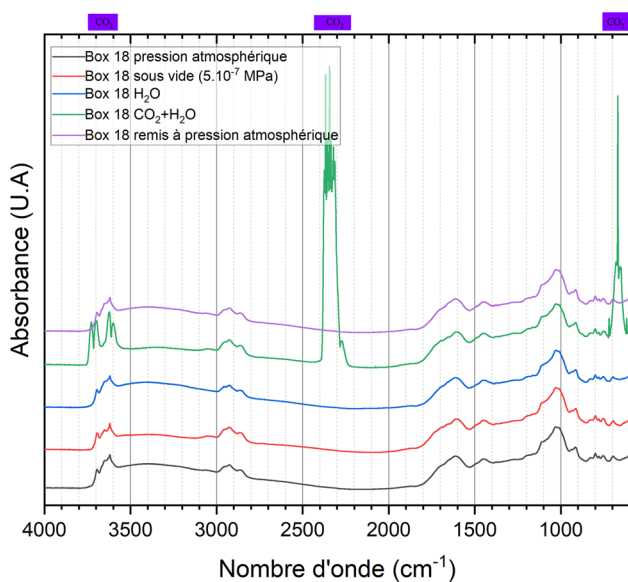


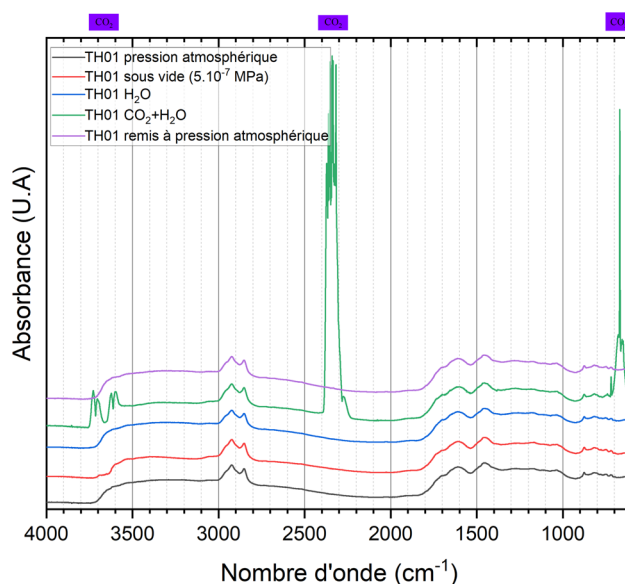
Fig. 7 IR spectra of sample TH01 under different gas flows (CO<sub>2</sub>, CH<sub>4</sub>) and at atmospheric pressure

Table 4 Positions and assignments of the absorption bands of Box 18 and TH01 coal samples

Spectral range (cm <sup>-1</sup> )	Functional group	Samples	
		Box 18 Peak positions (cm <sup>-1</sup> )	TH01 Peak positions (cm <sup>-1</sup> )
3750–3100	O–H in clay	3695	
		3649	
		3620	3616
3100–3000	O–H in water	3400	3306
	C–H in aromatic rings	3057	3062
3000–2800	–CH <sub>3</sub> and –CH <sub>2</sub> – in aliphatic compounds	2955	
		2927	2925
		2864	2851
		1750–1650	C=O
1650–1550	Aromatic ring	1653	1652
		1613	1610
1500–1450	C=C aromatic ring	1488	1490
		1447	1454
1460–1200	–CH <sub>2</sub> in aliphatic compounds, –C–O in aryl ethers, aliphatic ethers, alcohols, phenols	1451	1459
		1270	1279
		1183	1173
1200–900	–CH <sub>3</sub> in aliphatic compounds	1375	1377
		1104	1112
		1030	1036
		933	
900–600	Si–O kaolinite	914	913
	O–H kaolinite		
	C–H aromatic ring		



**Fig. 8** IR spectra of sample Box 18 under gas flows, gas humidified and at atmospheric pressure



**Fig. 9** IR spectra of sample TH01 under gas flows, gas humidified and at atmospheric pressure

the porosity in the coals is essentially due to the presence of micropores. Table 3 also shows that for different pore volumes ( $V_p$ ,  $V_M$  and  $V_m + V_\mu$ ), Box 18 values are larger than those of TH01 and the proportion of macropores lower than the total of mesopores and micropores. It is thus the latter that represents the bulk of the porosity of the studied coal samples. The total porosity of the studied coals comprises mainly free porosity. A high value indicates the presence of a weakly dispersed unimodal pore network and a random distribution of voids, favouring mercury withdrawal. The curves of first injections (Figs. 3 and 4) of mercury provide pores size distribution. Mesopores dominate the porosity of both coals as shown in Figs. 3 and 4. However, the estimated values of  $V_m + V_\mu$  in Table 3 showed a co-dominance of mesopores and micropores in the porosity of the coals studied. Indeed, the maximum mercury intrusion in the studied samples (Box 18 and TH01) is reached in the range of radii assigned to the mesopores. The unlooped pore distribution histograms are related to the fact that the porosimeter is at the limits of the pore radii (Hg pressure) that it can reach. Thus, it is likely that the porosity values are underestimated because it is not possible to access all the mesopores and micropores with the mercury porosimeter.

### 3.1.3 Functional groups of coal samples

Figure 5 shows DRIFT spectra of the two studied samples at the atmospheric pressure. The coal samples mainly present absorption bands of hydroxyl groups, aliphatic groups, oxygen-containing hydrocarbons and aromatic groups

and their corresponding assignments are listed in Table 4. Numerous bands are present on the two samples indicating the presence of functional groups such as O–H, C–H,  $\text{CH}_2$ ,  $\text{CH}_3$ , C=C, C=O and C–O. The large band centered around  $3400\text{ cm}^{-1}$  corresponds to the stretching vibration of liquid water contained in the coal. Among all the functional groups, oxygen-containing groups are particularly useful for bonding between gas and coal. Indeed, these functional groups are preferential adsorption sites for  $\text{CO}_2$  (Gao and Wang 2021; Gensterblum et al. 2014; Nishino 2001). They therefore influence the adsorption capacity and contribute to the good affinity of  $\text{CO}_2$  for the coal. Their significant presence in the two samples is an asset for  $\text{CO}_2$  storage.

The bands attributed to the  $-\text{CH}_2$  groups ( $2925$  and  $2851\text{ cm}^{-1}$ ) are more intense on the spectrum of TH01 than on that of Box 18. The  $-\text{CH}_3$  group vibrations appear as shoulder ( $2955\text{ cm}^{-1}$ ) on the spectrum of TH01. This means that the aliphatic chains are longer in TH01 than in Box 18 or that the aliphatic chains are more branched in Box 18 than in TH01. The band around  $3057\text{ cm}^{-1}$  corresponds to the stretching C–H bonds in the aromatic rings. The intensity of the bands assigned to the C–H aromatic bonds (around  $3060\text{ cm}^{-1}$ ) and C=C aromatic bonds (around  $1600\text{ cm}^{-1}$ ) is higher for Box 18 than for TH01 indicating a higher aromatic content in Box 18. The spectral profile of aliphatic  $\text{CH}_3$  and  $\text{CH}_2$  bands ( $3000$ – $2800\text{ cm}^{-1}$ ) and aromatic CH bands ( $900$ – $700\text{ cm}^{-1}$ ) can be used to calculate the degree of aromaticity and identify the coal maturity (Wang et al. 2021). It shows that the Box 18 sample is more mature than the TH01 sample.

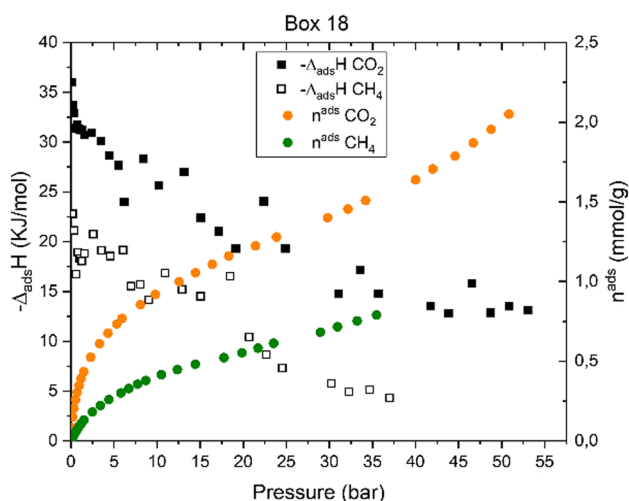


**Fig. 10** Adsorption isotherms and corresponding enthalpies of CO<sub>2</sub> and CH<sub>4</sub> on Box 18 sample (30 °C, 50 bars)

The samples also contain minerals compounds. Indeed, the Si–O or Al–O groups (bands between 1200 and 1000 cm<sup>-1</sup>) indicate the presence of silico-aluminates such as kaolinite (O–H bending bands at 933 and 914 cm<sup>-1</sup>). The characteristic bands of the O–H stretching vibrations (3695, 3649 and 3620 cm<sup>-1</sup>) of kaolinite are particularly visible on the Box 18 sample. The TH01 sample shows the presence of chlorite (3535 cm<sup>-1</sup>).

Figures 6 and 7 show the DRIFT spectra of Box 18 and TH01 coal samples respectively. For each sample, IR spectra are realised at atmospheric pressure and under primary vacuum ( $5 \times 10^{-7}$  MPa) to degas the sample before gas injection. The IR spectra are then recorded after adsorption of the gases (CH<sub>4</sub>, CO<sub>2</sub>) and also after the sample has been returned to the atmosphere to permit the desorption of the adsorbed gas. The vibrational–rotational bands of CO<sub>2</sub> (overtones: 3800–3550 cm<sup>-1</sup>, stretching: 2450–2250 cm<sup>-1</sup>, bending: 750–600 cm<sup>-1</sup>) and CH<sub>4</sub> (stretching: 3200–2800 cm<sup>-1</sup>, bending: 1400–1200 cm<sup>-1</sup>) are visible in the IR spectra of gas-saturated coal samples. However, after release to the atmosphere (desorption), the characteristic bands of the gases completely disappear and no modification of bands is observed compared to those of the initial samples (before gas saturation). There is therefore a reversibility of the interaction between the gas molecules and the coal. Thus, a physisorption of CO<sub>2</sub> and CH<sub>4</sub> seems to be observed.

Figures 8 and 9 show DRIFT spectra recorded on the Box 18 and TH01 samples during humidified CO<sub>2</sub> injections, the objective is to study the influence of water on the functional groups of coal. The reversibility of the interactions between the gas molecules and the coal is confirmed because the CO<sub>2</sub> bands initially present on the samples after adsorption, disappear on the samples returned to the

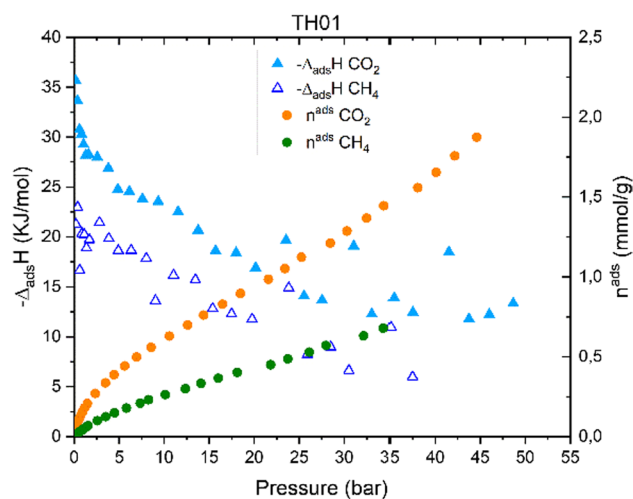


**Fig. 11** Adsorption isotherms and corresponding enthalpies of CO<sub>2</sub> and CH<sub>4</sub> on TH01 sample (30 °C, 50 bars)

atmosphere. The same results are obtained for CH<sub>4</sub>. However, a slight increase in the intensity of the large band of water (3750–3100 cm<sup>-1</sup>) is observed during the injection of the wet gas, indicating that water adsorbs onto the coal samples. Under primary vacuum, the OH band of water decreases slightly just as during the passage of the coal at atmospheric pressure and during the simultaneous injection of wet gas (CO<sub>2</sub> + H<sub>2</sub>O). These observations are identical in the case of wet CH<sub>4</sub> injection.

## 3.2 Adsorption results

### 3.2.1 Adsorption equilibrium analysis and enthalpies of adsorption

The CO<sub>2</sub> and CH<sub>4</sub> sorption isotherms on dry coals are given in Figs. 10 and 11. For the two samples, the carbon dioxide isotherms are systematically higher than the methane isotherms; the adsorption capacity of CO<sub>2</sub> is greater than of CH<sub>4</sub> (2.1 and 1.98 times for Box 18 and TH01 respectively). Main differences between the coals are concavity of the isotherm curves at low pressure and the CO<sub>2</sub> adsorbed amount at saturation. The Box18 sample has the highest amount of CO<sub>2</sub> adsorbed. Moreover, the CO<sub>2</sub> adsorption at lower pressure is much stronger than for TH01 sample. The same conclusion is made with CH<sub>4</sub> adsorption.

In parallel, the values of adsorption enthalpies obtained by calorimetry are given in Figs. 10 and 11. For CO<sub>2</sub>, they are 36.00 and 37.50 kJ/mol respectively for Box 18 and TH01 while for CH<sub>4</sub> they are 22.80 and 21.25 kJ/mol respectively for Box 18 and TH01. Those of CO<sub>2</sub> are clearly higher than those of CH<sub>4</sub>, which is a good indication in favor of CO<sub>2</sub> storage and CH<sub>4</sub> recovery (Table 5). The calorimetric



**Table 5** Adsorption isotherms parameters

Parameter	Box 18 (CO <sub>2</sub> )	TH01 (CO <sub>2</sub> )	Box 18 (CH <sub>4</sub> )	TH01 (CH <sub>4</sub> )
Langmuir model				
$R^2$	0.9757	0.9114	0.9794	0.9119
$\alpha_L$	0.2600	0.1000	0.1100	0.0500
$q_m$ (mmol/g)	1.3500	1.2300	0.7100	0.6300
Tóth model				
$R^2$	0.9983	0.9933	0.9940	0.9935
$n$	0.1800	0.2000	0.3800	0.1300
$\alpha_T$	1.2100	0.0400	0.0600	0.0000
$q_m$ (mmol/g)	1.8300	1.6400	0.9000	0.8900

$q_m$ : monolayer coverage;  $\alpha_L$ : Langmuir affinity;  $\alpha_T$ : Tóth affinity;  $n$ : heterogeneity index

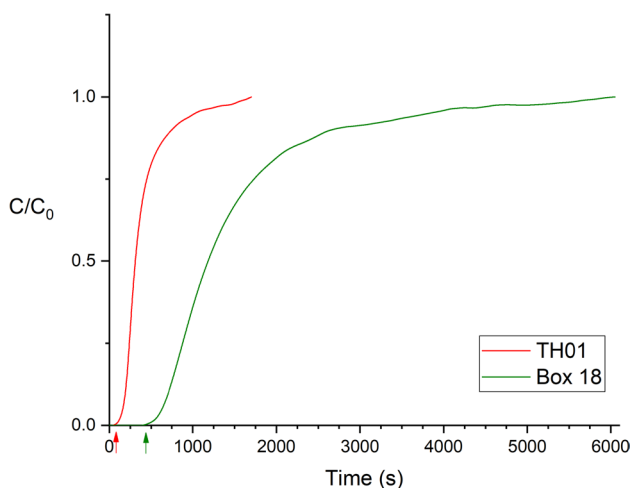


**Fig. 12** CO<sub>2</sub> breakthrough curves of coal samples

curves indicate that the adsorption enthalpies progressively decrease with increasing gas pressure until they stabilise at around 15 kJ/mol for CO<sub>2</sub> and 5 kJ/mol for CH<sub>4</sub>. In other words, the heat of adsorption released because of the adsorption is not the same during the filling of the adsorption sites of the coal samples.

### 3.2.2 Adsorption capacity of dry/wet coal samples

To study the effect of humidity on coal, breakthrough curves were determined at atmospheric pressure and ambient temperature. In Fig. 12 is given the comparative breakthrough curves of Box 18 and TH01 coals in fixed bed columns. The data were collected by micro-GC and the initial CO<sub>2</sub> concentration ( $C_0$ ) is 0.4%. Note that ( $C$ ) is the gas concentration analyzed at the reactor outlet by the micro-GC. Breakthrough occurred early for TH01 compared with Box18. A

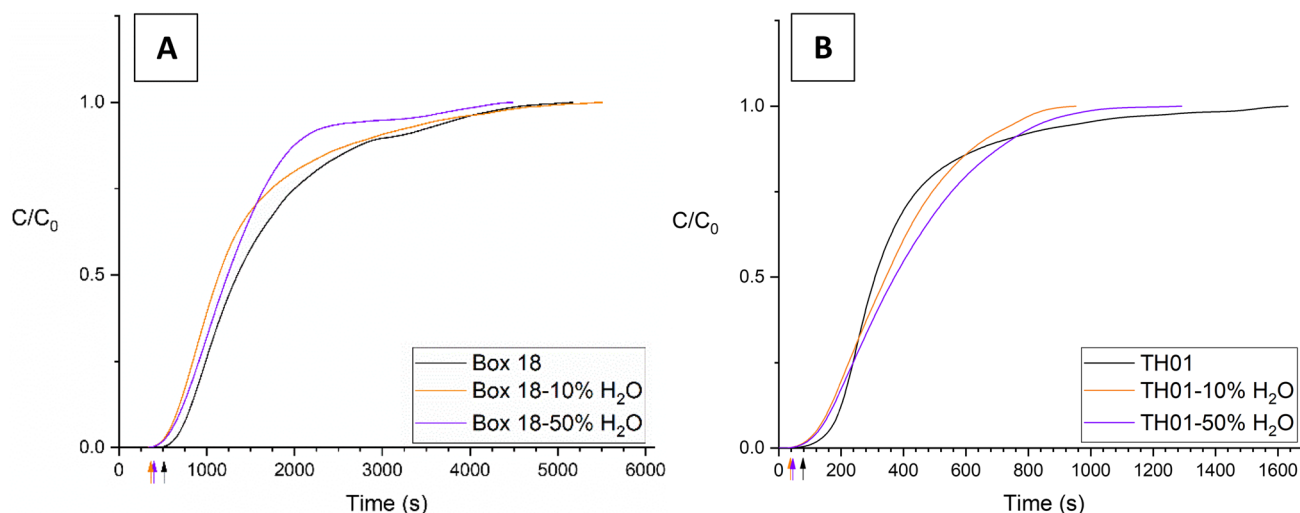


**Fig. 13** a CO<sub>2</sub> breakthrough curves for dry and wet Box 18 sample b CO<sub>2</sub> breakthrough curves for dry and wet TH01 sample

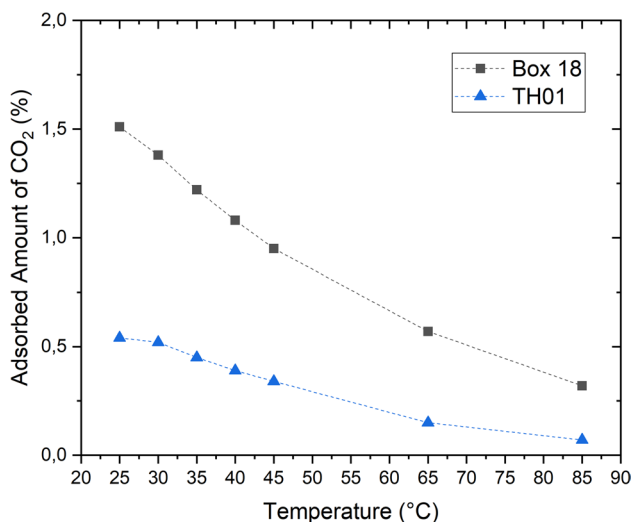


**Fig. 14** Quantities of CO<sub>2</sub> adsorbed as a function of temperature obtained by ATG (thermo-gravimetric analysis) at atmospheric pressure

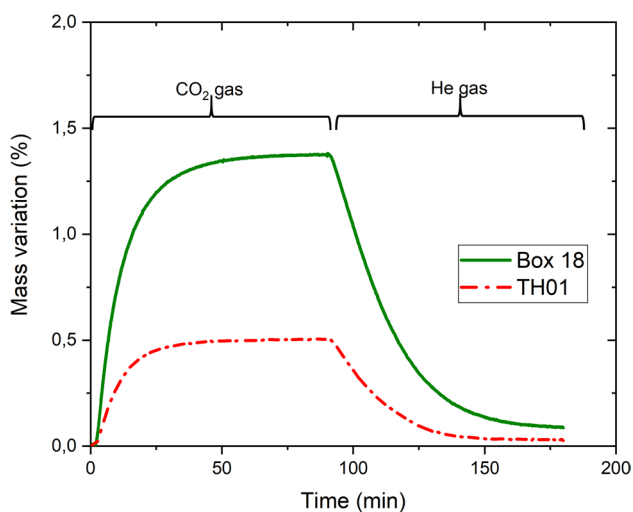


**Fig. 15** Mass variation of coals determined by thermogravimetric analyses under flow of CO<sub>2</sub> following by He (30 °C)

longer breakthrough time of 600 s for Box18 is recorded, whereas breakthrough occurring at 150 s for TH01. A longer breakthrough time corresponding to Box18 sample contributes to high adsorption CO<sub>2</sub>/g adsorbent.

Figure 13a shows the effect of humidity on box18 coal. As the percentage of humidity increases, the breakthrough time decreases (400 s) and the amount of CO<sub>2</sub> adsorbed also decreases slowly. The same behavior is observed with the TH01 coal (Fig. 13b). Moreover it can be seen that Box 18 adsorbs much more CO<sub>2</sub> than TH01 at different moistures (Figs. 13a, b).

### 3.2.3 Adsorption capacity of coal samples at different temperatures

The temperature increases with the depth of coal seams. It is therefore important to evaluate its impact on coals for which an ECBM-type operation is envisaged. Thermogravimetric analyses (TGA) were used to quantify the CO<sub>2</sub> adsorption capacity of the samples at different temperatures. For all the applied temperature at atmospheric pressure, the Box 18 systematically adsorbs much more CO<sub>2</sub> than TH01. The adsorbed amount of CO<sub>2</sub> decreases with the increase of temperature for both samples (Fig. 14). The adsorption capacities are reduced by 79% for Box 18 and 87% for TH01 respectively with increasing temperature (25–85 °C) (Fig. 14).

During the desorption phase under an inert gas (Helium), at constant temperature (30 °C), a return to the mass at 0% is not observed. Then, a part of the CO<sub>2</sub> adsorbed remains chemisorbed on the surface of the coal (Fig. 15). The samples desorb more than 94% of the CO<sub>2</sub> they have adsorbed (physisorption) and about 6% of the CO<sub>2</sub> remains bound to the coal after the passage of the He which desorbs the CO<sub>2</sub> (chemisorption). Thermogravimetric analyses have made it possible to evaluate these two types of gas–coal bonds in the samples studied. The quantities of CO<sub>2</sub> adsorbed from the Folschviller sample are about 3 times greater than those from the La Houve sample (Fig. 15). The slope of the mass uptake for Box 18 is much more important indicating a faster kinetic of adsorption. For example, 0.5% is the maximum adsorbed quantity for TH01 which is reach in about 25 min compared to about 5 min necessary to reach the same value for Box18 indicating a better accessibility to the pore network (Fig. 14).

## 4 Discussion

### 4.1 Physico-chemical properties, pores network and storage capacity of coals

The Folschviller sample (Box18) differs from the La Houve sample (TH01) in terms of porosities (total, free, trapped and helium accessible) (Table 3). The dominance of mesopores and micropores in the studied coals samples is in agreement with their maceral level. In fact, according to Table 1, all studied samples are dominated by vitrinite (> 47 vol%) and inertinite (> 26 vol%). Vitrinite is a mineral that affects the pore structure of coal, specifically the micropores and pore distribution, whereas inertinite contains more macropores and fewer micropores (Bustin and Clarkson 1998; Shen et al. 2019; Unsworth et al. 1989). The greater volume of voids in the Folschviller sample can be explained by its higher vitrinite content than in the La Houve sample. Indeed, the higher void volume of a coal is closely related to its high vitrinite content (Rodrigues and Lemos de Sousa 2002). It

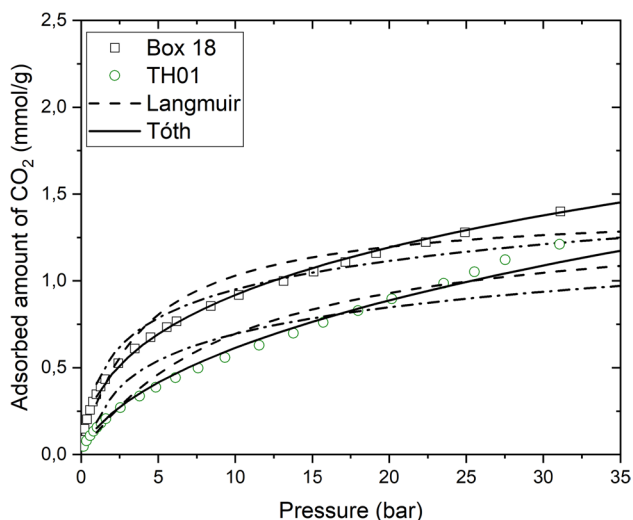


**Fig. 16** Adsorption isotherms of CO<sub>2</sub> onto coal samples at 30 °C: experimental data (points), fitted curve by Langmuir (dotted line) and Tóth (solid line) models

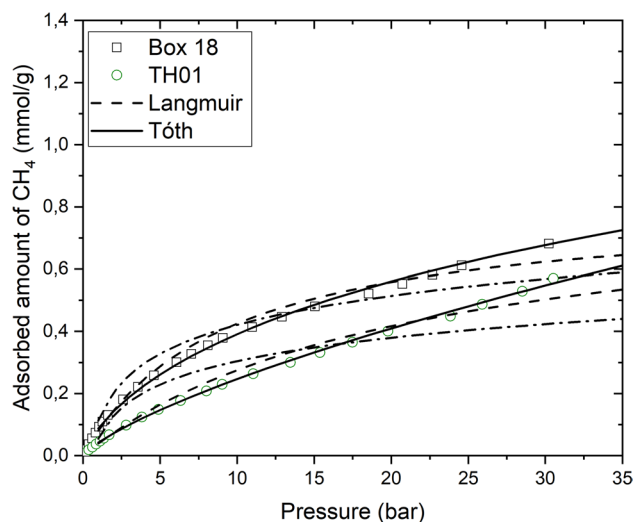


**Fig. 17** Adsorption isotherms of CH<sub>4</sub> onto coal samples at 30 °C: experimental data (points), fitted curve by Langmuir (dotted line) Tóth (solid line) models

is visible that the total porosity  $n_t$  (Eq. 1) and the helium accessible voids  $\varepsilon$  (Eq. 3), which are of the same order of magnitude, are quite different from the values obtained with mercury porosimetry. This could be explained by a scaling effect related to the difference in sample size and fracture density of the samples. Indeed, the samples used for mercury porosimetry had a volume of 1 cm<sup>3</sup> while the cores used for estimation of the bulk dry density (and then  $n_t$ ) had a volume of about 80 cm<sup>3</sup>. Since the fracture density is reduced as the volume of the sample decreases, the proportion of void will decrease following the same trend, thus considerably reducing the porosity of the material from one technique to the other.

The observation of mesopores and micropores volume (Table 3) and CH<sub>4</sub> adsorption enthalpies (Figs. 10 and 11) of the studied samples indicates a certain correlation. Indeed, the Folschviller sample (Box 18) which has the largest mesopores and micropores volume has also the highest CH<sub>4</sub> adsorption enthalpy. This shows the impact of the coal mesopores and micropores in the adsorption of CH<sub>4</sub>. This is in agreement with the positive correlation between pore volume and heat of adsorption of CH<sub>4</sub> found in the work of Li et al. (2021) on the effects of pore structure of coals of different ranks on the heat of adsorption of CH<sub>4</sub>.

The higher gas adsorption capacity (CO<sub>2</sub>/CH<sub>4</sub>) of the Box 18 sample can be explained by the porosity (percentage of void) contained in this coal. Indeed, the Box 18 sample contains voids (total porosity  $n_t$  and helium accessible pores) between 6 and 11 times higher than the La Houve sample, which allows him to have more storage space for gases (CO<sub>2</sub>/CH<sub>4</sub>) (Tables 2 and 3). In addition, the mesopores

and micropores volume of the Box 18 sample is 15 times larger than those of the TH01 sample (Table 3). Pore filling being the process by which gas incorporates the coal for storage, a coal will be all the more suitable for CO<sub>2</sub> storage as it will have a large amount of void (pores). Moreover, the mesopores and micropores are the places in which the majority of the adsorption phenomenon occurs, a large volume of the latter two constitutes an asset for the storage.

#### 4.2 Filling of the adsorption sites and isotherm modelling at 30 °C

The shape of the calorimetric curves (Figs. 10 and 11) suggests both an interaction of the molecules (CO<sub>2</sub>/CH<sub>4</sub>) with a heterogeneous surface (adsorbent) and a progressive filling of the pores from the smallest to the largest (Llewellyn and Maurin 2005). Indeed, if the coal is energetically heterogeneous due to a pore size distribution and/or a varying surface chemistry; initially, one would expect relatively strong interactions between the adsorbing molecules and the surface. The strength of these interactions will then decrease as these specific sites are occupied. Thus, for energetically heterogeneous adsorbents, a gradual decrease in the calorimetric signal is expected. Therefore, the measured heat decreases rapidly at first, but gradually with increasing adsorbed content (Deng et al. 2019). Moreover, for pressures higher than 30 bars we observe that the differential enthalpy of adsorption reduces to a value close to that of the CO<sub>2</sub> or CH<sub>4</sub> condensation enthalpy (about 17 kJ/mol for CO<sub>2</sub> and 8 kJ/mol for CH<sub>4</sub>). This can be assigned to adsorption completion or

filling of the meso/macropore volumes resulting in gas–gas interactions (Bourrelly 2006).

Based on the adsorption results at 30 °C, the adsorption isotherms were modeled between 0 and 30 bars. The Langmuir isotherm model was applied to estimate maximum adsorption capacity corresponding to complete monolayer coverage ( $q_m$ ) on the coal surface. In Figs. 16 and 17, Langmuir and Tóth models fitted results obtained on Box18 and TH01 coals are given. The gas affinities calculated from Langmuir ( $\alpha_L$ ) and Tóth ( $\alpha_T$ ) models show that the Folschviller sample has much higher affinities for CO<sub>2</sub> and CH<sub>4</sub> than the La Houve sample (Table 5). The Langmuir's model slightly overestimates the CO<sub>2</sub> and CH<sub>4</sub> adsorption for pressures below 25 bars. The Tóth model was also tested. While the use of the Langmuir's isotherm implies a homogeneous surface, the choice of the isotherm of Tóth suggests a heterogeneous surface if  $n \neq 1$ . The modelling carried out with the sorption isotherm data shows that the Tóth model is the one that describes well the adsorption of CO<sub>2</sub> and CH<sub>4</sub> of the studied samples and indicates that the adsorption surface is heterogeneous with an index  $n$  close to 0.2 for CO<sub>2</sub>. Concerning gases affinities, Box 18 sample has more affinity for CO<sub>2</sub> than TH01 sample. For methane, there are few differences between the affinities of the studied samples. The quantities of gas (CO<sub>2</sub>/CH<sub>4</sub>) adsorbed to the monolayer ( $q_m$ ) indicate that the values of Box 18 sample are higher than those of TH01 (Table 5).

### 4.3 Gas coal bonding

The adsorption of gas on coal is characterised by two types of bonding: physical adsorption (physisorption) and chemical adsorption (chemisorption). Chemisorption is characterized by high interaction potentials (ionic, metallic or chemical bonding) with hardly reversible or irreversible bonds. In the case of physisorption, the interactions involved are of the van der Waals type and of low energy with a reversible process. The gas–coal bonding of the samples was studied at low pressure by infrared analysis. The physisorption was identified by IR, spectra and the reversibility of the chemical bonding was achieved by venting to the atmosphere. These results are in agreement with the low-pressure data of Li et al. (2023) who studied the potential effect of CO<sub>2</sub> injection on the functional groups of medium-volatile bituminous coals. Nevertheless, their work showed irreversible effects of CO<sub>2</sub> at high pressures (7–8 MPa) on the C=O functional groups of these coals, raising questions about possible chemisorption in the interaction between CO<sub>2</sub> and coal. In addition,

Wang et al. (2017) also showed irreversible effects of CO<sub>2</sub> and CH<sub>4</sub> at high pressures (6 MPa) on the functional groups of the coals, which suggest chemical interactions at high pressure.

On the other hand, additional information was obtained with thermogravimetry. This is due to the small amount of chemisorbed CO<sub>2</sub> that was detected in addition to the proportion of physisorbed CO<sub>2</sub> detected predominantly in the coal (Fig. 15). The absence of chemisorption on the IR spectra could be explained by the fact that the proportion of chemisorption was too low and probably below the detection threshold of the infrared sensors.

The adsorption enthalpies values well below 200 kJ/mol obtained by calorimetry corroborate the physical adsorption observed on both the IR spectra and the thermogravimetric data (Figs. 10 and 11).

### 4.4 Comparative analysis of coal samples for use in CO<sub>2</sub>-ECBM

In a previous study, Defosse (2011) qualified the La Houve coal as one of the best candidates for CO<sub>2</sub>-ECBM after a comparison of numerous coal samples of various origins. This comparative analysis enabled him to highlight a certain number of criteria that a good candidate for CO<sub>2</sub>-ECBM must have. The feasibility of using the Folschviller sample (pilot site of the REGALOR project) will be studied on the basis of these criteria:

- (1) The percentage of ash. The two studied samples have low ash content (< 5%), so this is a positive point according to many authors who observed that ashes have negative impact on coal sorption capacity (Clarkson and Bustin 2000; Dutta et al. 2011).
- (2) The adsorption capacities. Folschviller coal sample (Box 18) adsorbs more CO<sub>2</sub> and CH<sub>4</sub> than TH01, so it is positive point for CO<sub>2</sub> storage and the available reserve of CH<sub>4</sub> to be exploited.
- (3) The gas–coal bond and gases affinities for coal. The samples studied have a weak energy bond with gases (CO<sub>2</sub>/CH<sub>4</sub>) corresponding to physisorption, nevertheless a low part of chemisorbed CO<sub>2</sub> could be detected. The Folschviller coal sample has a better affinity for carbon dioxide than the La Houve sample, making it much more suitable for storage. While both samples have a much lower affinity for methane than for carbon dioxide, suggesting a good methane recovery rate. From this comparison it can be seen that the Folschviller coal sample is also a good candidate for CO<sub>2</sub>-ECBM and is even better than the La Houve coal sample.



#### 4.5 Effect of water on adsorption capacity and O–H functional groups

ECBM is an operation in which methane is recovered by pumping and dewatering the coal seams. Then, it is important to study its influence on the adsorption capacity of CO<sub>2</sub> for possible storage. The values obtained for the CO<sub>2</sub> adsorption capacities (Figs. 13a, b) which show that dry coals adsorb more CO<sub>2</sub> than wet coals, are in agreement with that is generally observed in the literature (Gensterblum et al. 2014; Weishauptová et al. 2015). Gao and Wang (2021) and Švábová et al. (2012) explain this decrease in adsorption of wet coals by an occupation of CO<sub>2</sub> sorption sites by water molecules. Gensterblum et al. (2014) goes further by specifying a competition between water molecules and CO<sub>2</sub> for coal sorption sites. He indicated in his work that this competition is independent of gas type (CO<sub>2</sub>/CH<sub>4</sub>) and that a water molecule can occupy the site of one CH<sub>4</sub> molecule or the site of 2.2 CO<sub>2</sub> molecules. The process of occupancy of coal sorption sites by water molecules was presented by Charrière and Behra (2010). They showed from water sorption isotherms and calculated diffusion coefficients that water molecules adsorb on the primary sites of the coal (oxygen containing functional groups) before forming H<sub>2</sub>O clusters by coalescence and filling the micropores. The last two processes are slower than the first one. Liu et al. (2021) have demonstrated a decrease in the isosteric heat of water as a function of relative humidity, indicating that water adsorption on primary sites is controlled by the highest binding energy, while the interaction energy between water molecules during the cluster formation stage is relatively low. Liu et al. (2021) have also shown that the degree of oxidation dominates primary adsorption and, combined with the cumulative pore volume, determines secondary adsorption. Nishino (2001) had shown a positive correlation between the CO<sub>2</sub> adsorption capacity of carbons and the hydroxyl (OH) and carboxyl (COOH) functional groups. He highlighted in his work that CO<sub>2</sub> adsorption in the presence of water is related to the number of hydroxyl functional groups in the coal. From the above, it can be seen that the decrease in CO<sub>2</sub> adsorption from wet coals is related to a competition between water and gas for the OH and COOH adsorption sites of the coal.

The increase in the O–H band of water (Figs. 8 and 9) during the injection of wet gas onto the coal is in agreement with the work of Zhai et al. (2020) who showed that the presence of water increases the intensity of the IR absorbance of the O–H functional groups of coals. The suction created during vacuuming is responsible for the removal of water molecules from the surface of the coal and therefore for the decrease in intensity of the water O–H band

(3750–3100 cm<sup>-1</sup>). While the simultaneous injection of wet gas caused more interactions with the O–H band due to the presence of two adsorbates that are attracted to the hydroxyl functional groups of the coal (Charrière 2009).

#### 4.6 Effect of temperature on adsorption capacity

The decrease in CO<sub>2</sub> adsorption capacity with increasing temperature observed in this study (Fig. 13) is consistent with the work of (Busch et al. 2003; Charrière 2009; Guan et al. 2018; Krooss et al. 2002; Mabuza et al. 2022). These authors showed from the study of CO<sub>2</sub> sorption isotherms at different temperatures (from 10 to 70 °C) that the CO<sub>2</sub> adsorption capacity of coals decreases with increasing temperature. Indeed, during the adsorption process, an increase in temperature will lead the adsorbent-adsorbate system to a new state of thermodynamic equilibrium marked by the decrease of the adsorption capacity thus favoring the regeneration of the coal bed (Gabruś et al. 2021). Guan et al. (2018) furthermore highlighted a critical temperature (50 °C) above which the adsorbed amounts of gas remain constant with increasing temperature. For them, this phenomenon may be due to the influence of temperature on the molecular interaction between the adsorbate and the adsorbate. It should be noted that the critical temperature was not observed in this study and the hypotheses for this absence of critical temperature in the data can be various and varied. Indeed, the value of this critical temperature could be linked to the maturity, the origin or the quantity of coal analyzed.

The temperature effect was characterized by thermogravimetry because these analyses are faster and the results are comparable with those obtained on the adsorption isotherm at the same pressure. For instance, the adsorption isotherms obtained at 30 °C showed that the quantities adsorbed were 0.35 mmol/g for Box18 and 0.16 mmol/g for TH01 at 1 bar (Figs. 10 and 11). The values obtained by thermogravimetry are very close, 0.3 mmol/g and 0.11 mmol/g for Box 18 and TH01 respectively (Fig. 14).

## 5 Conclusions

A comparative study for CO<sub>2</sub>-ECBM recovery feasibility was performed on different coals from the Lorraine basin (France) using sorption isotherms, thermogravimetric analysis, and breakthrough curves. The volatile-rich bituminous coal from the Folschviller pilot site was compared to the sub-bituminous coal from the La Houve mine, which has already been identified as a good candidate for CO<sub>2</sub>-ECBM, and the following conclusions were drawn:

- (1) The adsorbed amounts of CO<sub>2</sub> obtained from sorption isotherms, breakthrough curves, and thermogravimetric data showed that Folschviller coal adsorbs more than the La Houve coal. This is due to the much higher void content (porosity and cracks) and gas affinity of the Folschviller coal, making it the best candidate for CO<sub>2</sub> storage. The same is true for CH<sub>4</sub>, suggesting a better CH<sub>4</sub> reserve for the Folschviller coal. The affinity of both coals for CO<sub>2</sub> is higher than for CH<sub>4</sub>, suggesting a good CH<sub>4</sub> recovery rate. Therefore, the Folschviller sample is also a good candidate for CO<sub>2</sub>-ECBM and is better than the La Houve sample.
- (2) The Tóth model better fits the adsorption isotherms of the two coals, reflecting the heterogeneity of their adsorption surfaces. The shape of the calorimetric curves indicates that the heterogeneity of the energy of the adsorption sites is due to the distribution of the pores and/or a variable surface chemistry.
- (3) The presence of oxygen-containing chemical functional groups in the IR spectra provides reassurance of the availability of preferential gas adsorption sites for the establishment of the gas–coal bond. The latter is of low energy (< 200 kJ/mol) corresponding to physical adsorption. Calorimetric adsorption enthalpies and IR spectra confirm this type of bond. Thermogravimetric data provided additional information on the presence of a very small amount of chemisorbed CO<sub>2</sub> (6%).
- (4) Breakthrough curves performed at atmospheric pressure showed that the water presence in the gas reduces the CO<sub>2</sub> adsorption capacity the two coals. Thermographic data obtained at atmospheric pressure showed that temperature reduces the CO<sub>2</sub> adsorption capacity of coals.

The combination of data from sorption isotherms, breakthrough curves and thermogravimetry has enabled us to gain a better understanding of the gas adsorption process (CO<sub>2</sub>/CH<sub>4</sub>) in the coal samples studied. Each of these analytical techniques provided specific information on gas adsorption, and comparison of the results obtained confirmed the affinities and quantities of adsorbed gases.

At present, there are very little data on coals from the Lorraine basin. The experimental results in this paper could serve as updated data for future research work that, for example, will take into account in situ constraints and the permeability of coals in order to optimize CO<sub>2</sub> injections and CH<sub>4</sub> recovery. These results could also help the large CO<sub>2</sub> emitters located in the Lorraine basin in their decision-making on how to reduce their CO<sub>2</sub> emissions into the atmosphere.

**Acknowledgements** This work was financed by the REGALOR project (Ressources Gazières de Lorraine). The authors would like to thank Aurélien Randi for his help in the technical maintenance of the gases.

## Declarations

**Competing interests** The authors declare that they have no known competing financial interests or personal relationships that could have appeared to influence the work reported in this paper.

**Open Access** This article is licensed under a Creative Commons Attribution 4.0 International License, which permits use, sharing, adaptation, distribution and reproduction in any medium or format, as long as you give appropriate credit to the original author(s) and the source, provide a link to the Creative Commons licence, and indicate if changes were made. The images or other third party material in this article are included in the article's Creative Commons licence, unless indicated otherwise in a credit line to the material. If material is not included in the article's Creative Commons licence and your intended use is not permitted by statutory regulation or exceeds the permitted use, you will need to obtain permission directly from the copyright holder. To view a copy of this licence, visit <http://creativecommons.org/licenses/by/4.0/>.

## References

- Bourrelly S (2006) Propriétés thermodynamiques de nouveaux matériaux nanoporeux hybrides organiques/inorganiques pour l'adsorption de gaz à effet de serre [These de doctorat, Aix-Marseille 1]. <https://www.theses.fr/2006AIX11061>
- Busch A, Krooss BM, Gensterblum Y, van Bergen F, Pagnier HJM (2003) High-pressure adsorption of methane, carbon dioxide and their mixtures on coals with a special focus on the preferential sorption behaviour. *J Geochem Explor* 78–79:671–674. [https://doi.org/10.1016/S0375-6742\(03\)00122-5](https://doi.org/10.1016/S0375-6742(03)00122-5)
- Bustin RM, Clarkson CR (1998) Geological controls on coalbed methane reservoir capacity and gas content. *Int J Coal Geol* 38(1):3–26. [https://doi.org/10.1016/S0166-5162\(98\)00030-5](https://doi.org/10.1016/S0166-5162(98)00030-5)
- Calvet E, Prat H (1958) Récents progrès en calorimétrie (Dunod). Dunod
- Charrière D (2009) Caractérisation de la sorption de gaz sur les charbons application au stockage géologique du dioxyde de carbone dans les veines de charbon. Université de Toulouse, Toulouse
- Charrière D, Behra P (2010) Water sorption on coals. *J Colloid Interface Sci* 344(2):460–467. <https://doi.org/10.1016/j.jcis.2009.11.064>
- Clarkson CR, Bustin RM (1999) The effect of pore structure and gas pressure upon the transport properties of coal: a laboratory and modeling study. 2. Adsorption rate modeling. *Fuel* 78(11):1345–1362. [https://doi.org/10.1016/S0016-2361\(99\)00056-3](https://doi.org/10.1016/S0016-2361(99)00056-3)
- Clarkson CR, Bustin RM (2000) Binary gas adsorption-desorption isotherms: effect of moisture and coal composition upon carbon dioxide selectivity over methane, 31
- Copard Y (2002) Altération diagénétique et post-diagénétique (thermicité, oxydation) des charbons carbonifères du Massif Central français (Saint-Etienne, Graissessac et autres lieux)
- Defossez P (2011) Caractérisation de charbons en vue de leur utilisation pour le stockage géologique de CO<sub>2</sub>. Université d'Orléans, Orléans

- Deng J, Kang J, Zhou F, Li H, Zhang D, Li G (2019) The adsorption heat of methane on coal: comparison of theoretical and calorimetric heat and model of heat flow by microcalorimeter. *Fuel* 237:81–90. <https://doi.org/10.1016/j.fuel.2018.09.123>
- Dutta P, Bhowmik S, Das S (2011) Methane and carbon dioxide sorption on a set of coals from India. *Int J Coal Geol* 85(3):289–299. <https://doi.org/10.1016/j.coal.2010.12.004>
- Gabruś E, Wojtacha-Rychter K, Aleksandrak T, Smoliński A, Król M (2021) The feasibility of CO<sub>2</sub> emission reduction by adsorptive storage on Polish hard coals in the Upper Silesia Coal Basin: an experimental and modeling study of equilibrium, kinetics and thermodynamics. *Sci Total Environ* 796:149064. <https://doi.org/10.1016/j.scitotenv.2021.149064>
- Gan H, Nandi SP, Walker PL (1972) Nature of the porosity in American coals. *Fuel* 51(4):272–277. [https://doi.org/10.1016/0016-2361\(72\)90003-8](https://doi.org/10.1016/0016-2361(72)90003-8)
- Gao ZH, Wang J (2021) Effect of low-concentration steam on carbon dioxide adsorption by bituminous coal. *AIP Adv* 11(1):015350. <https://doi.org/10.1063/5.0022861>
- Gensterblum Y, Busch A, Krooss BM (2014) Molecular concept and experimental evidence of competitive adsorption of H<sub>2</sub>O, CO<sub>2</sub> and CH<sub>4</sub> on organic material. *Fuel* 115:581–588. <https://doi.org/10.1016/j.fuel.2013.07.014>
- Godec M, Koperina G, Petrusak R, Oudinot A (2013) Potential for enhanced gas recovery and CO<sub>2</sub> storage in the Marcellus Shale in the Eastern United States. *Int J Coal Geol* 118:95–104. <https://doi.org/10.1016/j.coal.2013.05.007>
- Guan C, Liu S, Li C, Wang Y, Zhao Y (2018) The temperature effect on the methane and CO<sub>2</sub> adsorption capacities of Illinois coal. *Fuel* 211:241–250. <https://doi.org/10.1016/j.fuel.2017.09.046>
- Gunzburger Y (2016) The coal gas project in Lorraine and its integration in the territory (final report)
- Hayes K, Roeshot S (2014) The natural gas revolution: resource library. <https://www.rff.org/publications/reports/the-natural-gas-revolution-resource-library/>
- IUPAC (1972) International Union of pure and applied chemistry, manuals of symbols and terminology for physico chemical quantities and units (Butterworth)
- Izart A, Barbarand J, Michels R, Privalov VA (2016) Modelling of the thermal history of the Carboniferous Lorraine Coal Basin: consequences for coal bed methane. *Int J Coal Geol* 168:253–274. <https://doi.org/10.1016/j.coal.2016.11.008>
- Krooss BM, van Bergen F, Gensterblum Y, Siemons N, Pagnier HJM, David P (2002) High-pressure methane and carbon dioxide adsorption on dry and moisture-equilibrated Pennsylvanian coals. *Int J Coal Geol* 51(2):69–92. [https://doi.org/10.1016/S0166-5162\(02\)00078-2](https://doi.org/10.1016/S0166-5162(02)00078-2)
- Lafargue E, Marquis F, Pillot D (1998) Rock-eval 6 applications in hydrocarbon exploration, production, and soil contamination studies. *Rev L'inst Fr Pét* 53(4):421–437. <https://doi.org/10.2516/ogst:1998036>
- Langmuir I (1918) The adsorption of gases on plane surfaces of glass, mica and platinum. *J Am Chem Soc* 40(9):1361–1403. <https://doi.org/10.1021/ja02242a004>
- Li X, Fang Z (2014) Current status and technical challenges of CO<sub>2</sub> storage in coal seams and enhanced coalbed methane recovery: an overview. *Int J Coal Sci Technol* 1(1):93–102. <https://doi.org/10.1007/s40789-014-0002-9>
- Li H, Wang S, Zeng Q, Kang J, Guan W, Li W (2021) Effects of pore structure of different rank coals on methane adsorption heat. *Processes* 9(11):1971. <https://doi.org/10.3390/pr9111971>
- Li J, Pan J, Wang X, Wang K, Nie S, Gao D (2023) Potential effect of carbon dioxide injection on the functional groups of medium volatile bituminous coals analysed using in-situ diffuse reflectance Fourier-transform infrared spectroscopy. *Int J Coal Geol* 265:104169. <https://doi.org/10.1016/j.coal.2022.104169>
- Liu Z, Zhang Z, Choi SK, Lu Y (2018) Surface properties and pore structure of anthracite, bituminous coal and lignite. *Energies* 11(6):1502. <https://doi.org/10.3390/en11061502>
- Liu A, Liu S, Liu P, Wang K (2021) Water sorption on coal: effects of oxygen-containing function groups and pore structure. *Int J Coal Sci Technol* 8(5):983–1002. <https://doi.org/10.1007/s40789-021-00424-6>
- Llewellyn PL, Maurin G (2005) *Comptes rendus chimie*
- Mabuza M, Premlall K, Daramola MO (2022) Modelling and thermodynamic properties of pure CO<sub>2</sub> and flue gas sorption data on South African coals using Langmuir, Freundlich, Temkin, and extended Langmuir isotherm models. *Int J Coal Sci Technol* 9(1):45. <https://doi.org/10.1007/s40789-022-00515-y>
- Mahajan OP (1991) CO<sub>2</sub> surface area of coals: the 25-year paradox. *Carbon* 29(6):735–742. [https://doi.org/10.1016/0008-6223\(91\)90010-G](https://doi.org/10.1016/0008-6223(91)90010-G)
- Marsh H (1987) Adsorption methods to study microporosity in coals and carbons—a critique. *Carbon* 25(1):49–58. [https://doi.org/10.1016/0008-6223\(87\)90039-X](https://doi.org/10.1016/0008-6223(87)90039-X)
- Metz B, Davidson O, de Coninck H, Loss M, Meyer L (eds) (2005) IPCC special report on carbon dioxide capture and storage. Cambridge University Press, Cambridge, p 43. <https://doi.org/10.1021/cr2003272>
- Moroeng OM, Mhuka V, Nindi MM, Roberts RJ, Wagner NJ (2019) Comparative study of a vitrinite-rich and an inertinite-rich Witbank coal (South Africa) using pyrolysis-gas chromatography. *Int J Coal Sci Technol* 6(4):621–632. <https://doi.org/10.1007/s40789-019-00274-3>
- Mukherjee M, Misra S (2018) A review of experimental research on enhanced coal bed methane (ECBM) recovery via CO<sub>2</sub> sequestration. *Earth Sci Rev* 179:392–410. <https://doi.org/10.1016/j.earscirev.2018.02.018>
- Nishino J (2001) Adsorption of water vapor and carbon dioxide at carboxylic functional groups on the surface of coal. *Fuel* 80:757–764
- Okolo GN, Everson RC, Neomagus HWJP, Roberts MJ, Sakurovs R (2015) Comparing the porosity and surface areas of coal as measured by gas adsorption, mercury intrusion and SAXS techniques. *Fuel* 141:293–304. <https://doi.org/10.1016/j.fuel.2014.10.046>
- Ottiger S, Pini R, Storti G, Mazzotti M, Bencini R, Quattrocchi F, Sardu G, Deriu G (2006) Adsorption of pure carbon dioxide and methane on dry coal from the Sulcis coal province (SW Sardinia, Italy). *Environ Prog* 25(4):355–364. <https://doi.org/10.1002/ep.10169>
- Parkash S, Chakrabarty SK (1986) Microporosity in Alberta plains coals. *Int J Coal Geol* 6(1):55–70. [https://doi.org/10.1016/0166-5162\(86\)90025-X](https://doi.org/10.1016/0166-5162(86)90025-X)
- Pashin JC, Groshong RH Jr, Carroll RE (2001) Carbon sequestration potential of coalbed methane reservoirs in the Black Warrior basin: a preliminary look. In: Proceedings 2001 international coalbed methane, pp 51–62
- Poyet T (2002) Etude thermodynamique de l'adsorption des gaz sous pression par des tamis moléculaires. University of Provence (Aix-Marseille I)
- Premlall K, Mabuza M, Wagner N (2014) Evaluating CO<sub>2</sub> sorption capacity of a number of South African (SA) coal types: comparative study of the different coal properties at incremental pressures up to supercritical pressures. *Energy Procedia* 51:299–307. <https://doi.org/10.1016/j.egypro.2014.07.036>
- Rodrigues CF, Lemos de Sousa MJ (2002) The measurement of coal porosity with different gases. *Int J Coal Geol* 48(3–4):245–251. [https://doi.org/10.1016/S0166-5162\(01\)00061-1](https://doi.org/10.1016/S0166-5162(01)00061-1)
- Rouquerol J, Partyka S, Rouquerol F (1977) Calorimetric evidence for a bidimensional phase change in the monolayer of nitrogen or

- argon adsorbed on graphite at 77 K. *J Chem Soc Faraday Trans I Phys Chem Condens Phases* 73:306–314. <https://doi.org/10.1039/F19777300306>
- Shen J, Qin Y, Zhao J (2019) Maceral contribution to pore size distribution in anthracite in the South Qinshui Basin. *Energy Fuels* 33(8):7234–7243. <https://doi.org/10.1021/acs.energyfuels.9b01514>
- Shi J-Q, Durucan S (2005) A numerical simulation study of the Allison Unit CO<sub>2</sub>-ECBM pilot: the impact of matrix shrinkage and swelling on ECBM production and CO<sub>2</sub> injectivity. In: *Proceedings of the 7th International conference on greenhouse gas control technologies 5– September 2004, Vancouver, Canada*, pp 431–439. [https://hero.epa.gov/hero/index.cfm/reference/details/reference\\_id/6215310](https://hero.epa.gov/hero/index.cfm/reference/details/reference_id/6215310)
- Sing KSW (1995) Physisorption of nitrogen by porous materials. *J Porous Mater* 2(1):5–8. <https://doi.org/10.1007/BF00486564>
- Švábová M, Weishauptová Z, Příbyl O (2012) The effect of moisture on the sorption process of CO<sub>2</sub> on coal. *Fuel* 92(1):187–196. <https://doi.org/10.1016/j.fuel.2011.08.030>
- Tóth J (1962) Gas adsorption on solid surfaces of inhomogeneous activity. *Acta Chimica (Academiae Scientiarum) Hungaricae*
- Unsworth JF, Fowler CS, Jones LF (1989) Moisture in coal: 2. Maceral effects on pore structure. *Fuel* 68(1):18–26. [https://doi.org/10.1016/0016-2361\(89\)90005-7](https://doi.org/10.1016/0016-2361(89)90005-7)
- Wang K, Du F, Wang G (2017) The influence of methane and CO<sub>2</sub> adsorption on the functional groups of coals: insights from a Fourier transform infrared investigation. *J Nat Gas Sci Eng* 45:358–367. <https://doi.org/10.1016/j.jngse.2017.06.003>
- Wang C, Feng Z, Wang X (2021) Effect of functional groups in coal on the depth of adsorption potential well. *Adsorpt Sci Technol* 2021:e3820762. <https://doi.org/10.1155/2021/3820762>
- Weishauptová Z, Příbyl O, Sýkorová I, Machovič V (2015) Effect of bituminous coal properties on carbon dioxide and methane high pressure sorption. *Fuel* 139:115–124. <https://doi.org/10.1016/j.fuel.2014.08.030>
- White CM (2003) An initial set of working hypotheses concerning some chemical and physical events when CO<sub>2</sub> is injected into a coalbed. *Am Chem Soc Div Fuel* 46:114–116
- White CM, Smith DH, Jones KL, Goodman AL, Jikich SA, LaCount RB, DuBose SB, Ozdemir E, Morsi BI, Schroeder KT (2005) Sequestration of carbon dioxide in coal with enhanced coalbed methane recovery—a review. *Energy Fuels* 19(3):659–724. <https://doi.org/10.1021/ef040047w>
- Zhai X, Ge H, Wang T, Shu C-M, Li J (2020) Effect of water immersion on active functional groups and characteristic temperatures of bituminous coal. *Energy* 205:118076. <https://doi.org/10.1016/j.energy.2020.118076>
- Zhang Q, Yang X (1999) Isothermal adsorption of coals on methane under equilibrium moisture. *Mei t'an Hsueh Pao J China Coal Soc* 24:566–570

**Publisher's Note** Springer Nature remains neutral with regard to jurisdictional claims in published maps and institutional affiliations.